American Mineralogist, Volume 77, pages 251–257, 1992

Crystal-field spectroscopic study of Cr-doped mullite

Ko Ikeda
Department of Advanced Materials Science and Engineering, Yamaguchi University, 755 Ube, Japan
Hartmut Schneider
DLR Institute for Materials Research, D-5000 Köln 90, Germany
Masahide Akasaka
Department of Geology, Shimane University, 690 Matsue, Japan
Helmut Rager
Department of Geosciences, University of Marburg, D-3550 Marburg, Germany

Abstract

Unpolarized crystal-field spectra were measured in the wavelength range of 340 to 1540 nm by reflection from mullite powders. The mullite sample contained 8.1 wt% Cr_2O_3 and was synthesized by reaction sintering from Al_2O_3, SiO_2, and Cr_2O_3 powders. The spectra were converted to wavenumber scale and were interpreted by curve fittings, applying Gaussian functions. The results yielded two pairs of absorption peaks. One of them is attributed to Cr^{3+} ions replacing octahedral Al^{3+} ions. The other pair of absorption peaks is assigned to Cr^{3+} ions occurring at interstitial octahedral sites.

Introduction

Mullite is considered to be a candidate for advanced ceramics for use at high temperature because mullite matrix materials exhibit low thermal expansion, very low thermal conductivity, and excellent creep resistance. Mullite has the general formula $Al_{4+2x}Si_{2-2x}O_{10-x}$ ($0.2 \leqq x \leqq 0.5$) (Durovič, 1969; Cameron, 1977; Schneider, 1986) with the most frequently occurring compositions at about $x = 0.25$ (⅔ mullite: $3Al_2O_3 \cdot 2SiO_2$) and $x = 0.40$ (⅘ mullite: $2Al_2O_3 \cdot SiO_2$). Study of phase equilibria yielded a solid-solution field of mullite in the system Al_2O_3-SiO_2 at high temperature (Aramaki and Roy, 1962; Pask, 1990; Klug et al., 1990). Recently it was reported that mullite can contain up to 84 wt% Al_2O_3, nearly corresponding to ⅘ mullite (Klug et al., 1990). Solid solution between sillimanite ($x = 0$) and ½ mullite ($x = 0.25$), which was studied by Hariya et al. (1969), seems to be possible at elevated pressure only.

The average mullite structure has space group *Pbam* and is characterized by chains of Al-O octahedra (designated as M1) and double chains of Al,Si-O tetrahedra extending parallel to the **c** axis. The M1 octahedra are relatively regular in shape with a mean M-O distance of 1.911 Å. The tetrahedra are classified into two groups: one of them contains Si^{4+} and Al^{3+} ions (designated as M2). The other contains only Al^{3+} ions and is associated with O(C) O vacancies (designated as Al*). The Al* tetrahedra have somewhat longer mean M-O distances than the M2 tetrahedra (1.803 Å instead of 1.702 Å, Saalfeld and Guse, 1981; Burnham, 1963; Sadanaga et al., 1962). M1 octahedra and M2 and Al* tetrahedra have point symmetries $C_{2h}(2/m)$, $C_s(m)$ and $C_s(m)$, respectively. Within the polyhedral chains O(C) O vacancies occur that balance the charge deficiency due to varying Al,Si ratios, as seen in Figure 1. These O(C) O vacancies occur on the average after every fifth O(C) atom for ⅘ mullite and after every eighth for ⅔ mullite in the **c** direction. Because of the presence of O(C) vacancies the channels are disturbed, leaving a vacancy.

Saalfeld (1979), McConnell and Heine (1985), Angel and Prewitt (1987), and Morimoto (1990) demonstrated that an incommensurate structure with modulation of two sets of ordering patterns with different symmetries occurs. Both sets have chains of M1 octahedra parallel to **c**. In one case, the chains of octahedra are connected by tetrahedral double chains with all tetrahedra being cross linked by O(C) bridging atoms, as in sillimanite. In the other case, each second tetrahedra pair points away from the double chain, producing Al* tetrahedra. This structural arrangement resembles that of ι alumina.

The mullite structure is able to incorporate considerable amounts of transition metal ions. The most important species are Ti^{3+}, Ti^{4+}, V^{3+}, V^{4+}, Cr^{3+}, Mn^{3+}, and Fe^{3+} ions (Schneider, 1990). In a recent study, solubility of up to 12 wt% Cr_2O_3 has been found (Rager et al., 1990). According to EPR spectroscopic studies, Rager et al. suggested that Cr^{3+} enters M1 octahedra and octahedral interstices in the channels or O vacancies occurring in the mullite structure. Crystal-field spectroscopic studies were carried out in order to provide further information on the distribution of Cr in the mullite structure.

Experimental

Mullite samples were synthesized by the reaction sintering technique. Chemically pure α-Al_2O_3 (54.5 wt%),

0003–004X/92/0304–0251$02.00

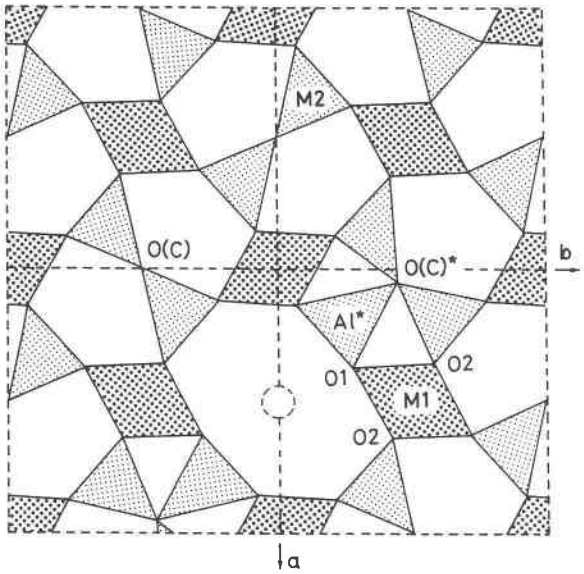

Fig. 1. Schematic drawing of the crystal structure of mullite in a view down the c axis.

α-SiO_2 (38.0 wt%), and Cr_2O_3 (7.5 wt%) powders were used for the syntheses. After grinding the starting powders with ethyl alcohol in an agate mortar, the mixture was annealed in a PtRh crucible at 1650 °C for 10 d. The grain boundary glass present after the reaction sintering process was leached with an HF/HCl acid solution. Since the microprobe studies yielded no evidence for the occurrence of any glass within the mullite crystals, the material can be considered to be single-phase mullite after acid treatment. Electron microprobe analysis of the sample showed that the mullite was approximately of ⅔-type composition, containing 8.1 wt% Cr_2O_3 and 0.1 wt% Fe as Fe^{3+} (Table 1).

The acid-treated mullite powders are of green color and were checked prior to spectroscopic measurements with the polarizing microscope and by X-ray diffraction. No impurity minerals or glass were observed in the samples so analyzed.

Unpolarized crystal-field spectra were measured in the wavelength range from 340 nm (29400 cm^{-1}) to 1540 nm (6500 cm^{-1}) using a Hitachi 323S automatic recording spectrophotometer. A white plate of barium sulphate was used as reference. Applying the Kubelka-Munk formula, the reflectance spectra obtained were converted to absorption spectra on a wavenumber scale with 100 cm^{-1} intervals. Curve fittings were performed on a personal computer, applying Gaussian functions. Spin-forbidden energy levels were neglected because no traces of these levels were observed in the spectrum. These levels generally show line spectra of weak intensity for $^{[6]}Cr^{3+}$ and probably do not appreciably influence the results.

Results

The assignments of absorption bands have been carried out assuming cubic site symmetry $O_h(m3m)$ for all Cr centers. Although Cr may occur in several valence states (see Rager et al., 1990), only the trivalent state was considered because the spectra gave no indication of Cr ions different from Cr^{3+}.

Table 1. Chemical composition and cell dimensions of mullite

Oxide component	Al_2O_3	Cr_2O_3	Fe_2O_3	SiO_2
Composition (wt%)	63.7	8.1	0.1	28.1
Molar ratio	←	2.9	→	2.0

Chemical formula $(Al_{0.823}Fe^{3+}_{0.002}Cr^{3+}_{0.175})(Al_{1+x}Si_{1-x})_2O_{5-x/2}$*

Cell dimensions (Å) $a = 7.559(2)$ $b = 7.702(2)$ $c = 2.896(1)$

* The $x = 0.231$; Cr and Fe are assumed as octahedral and trivalent.

Electron configuration and energy diagram

As can be seen in Figure 2, three types of electron configurations are associated with octahedrally coordinated and tetrahedrally coordinated trivalent Cr. Octahedral coordination has only one type since there is no distinction between the high spin state and the low spin state, whereas tetrahedral coordination may have the high spin state or the low spin state. The tetrahedrally coordinated high spin state is less stable because of smaller CFSE (crystal-field stabilization energy). The tetrahedrally coordinated low spin state is stable at low temperatures and becomes unstable at high temperatures as a result of site expansion (Ikeda and Yagi, 1982). The higher the temperature the more likely the $^{[4]}Cr^{3+}$ will be found in the high spin state. However, this state is unstable and the Cr^{3+} eventually becomes highly stabilized in octahedral sites at high temperatures. Consequently, the spectra may be analyzed assuming octahedral coordination.

For octahedrally coordinated trivalent Cr there are three spin-allowed transitions as shown in Figure 3. Usually only the two lower ones are observed, whereas the third transition often overlaps with charge transfer bands located in the ultraviolet region, as stated elsewhere. Sometimes, spin-forbidden transitions of very weak intensity are observed.

The crystal-field spectrum of the Cr-doped mullite is shown in Figure 4. Generally, octahedrally coordinated Cr^{3+} ions give rise to two main absorption bands belonging to spin-allowed transitions, $^4T_{2g} \leftarrow {}^4A_{2g}$ and $^4T_{1g} \leftarrow {}^4A_{2g}$ of the F term. The experimental crystal-field spec-

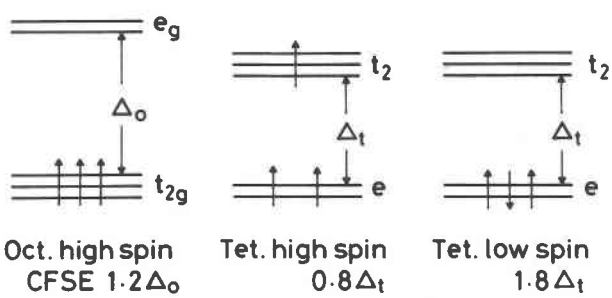

Fig. 2. Electron configurations of trivalent Cr.

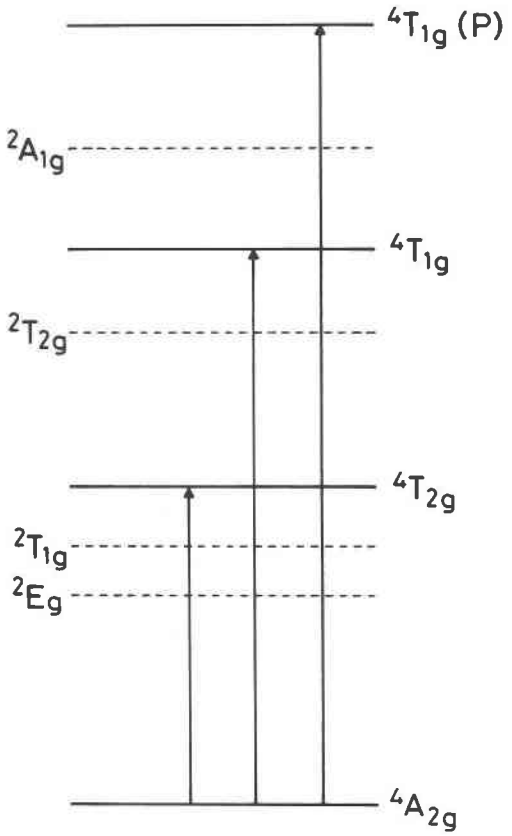

Fig. 3. Schematic energy diagram of octahedrally coordinated trivalent Cr.

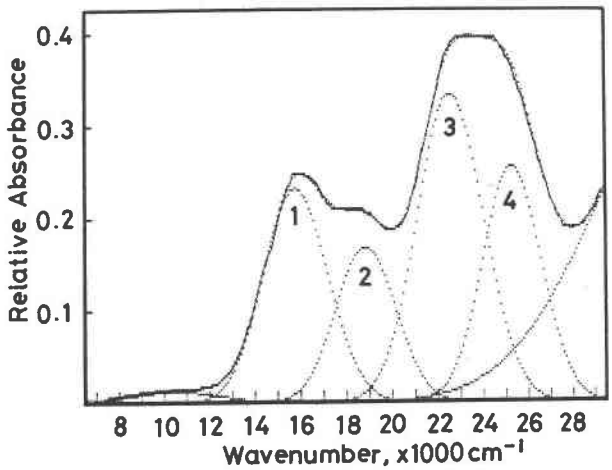

Fig. 4. Crystal-field spectrum of chromium mullite and the results of curve fittings. The 1-3 pair is assigned to channel octahedra, the 2-4 pair to M1 octahedra. The sum of the Gaussian functions is shown along the solid curve as dots. The broad absorption of low-intensity centering at 10500 cm^{-1} is due to the presence of traces of octahedrally coordinated Fe^{2+}.

trum consists of three main bands, including the middle steplike shoulder of lower intensity, as seen in Figure 4. If it is supposed that the bands at approximately 16000 cm^{-1} and 23500 cm^{-1} belong to the two spin-allowed transitions of a single Cr^{3+} center in mullite, the band at approximately 19000 cm^{-1} cannot be assigned to that center, even if it is a spin-forbidden band. The band at approximately 23500 cm^{-1} is a double band, judging from the flatness and broadening of the peak. Peak splitting and broadening caused by site distortions from cubic symmetry are generally considered to be approximately 1000 cm^{-1}, and even for Jahn-Teller species, for instance octahedral Cu^{2+} ions, they are 2000 cm^{-1} at most (Figgis, 1969). Octahedral Cr^{3+} ions are not Jahn-Teller species in the ground state (Earnshaw, 1970). Excited states correspond to the Jahn-Teller effect (Kettle, 1972; Burns, 1972), but large peak splittings for Cr^{3+} ions resulting from this effect have never been found; this is unlike Fe^{2+} ions, for which approximate splitting of 5500 cm^{-1} was observed for a very distorted M4 site of amphibole (Goldman and Rossman, 1977). The observed splitting magnitude of approximately 3000 cm^{-1} therefore cannot be due to a single site. We believe instead that two Cr^{3+} sites with slightly different distortions must be taken into account.

Curve fittings and assignments

Results of curve fittings by Gaussian functions and assignments are shown in Figure 4 and Table 2. The first IR overtone of absorbed H_2O of low intensity observed around 6900 cm^{-1} was corrected by smoothing. According to Beales and Day (1980), the first overtone of OH in glass is located at 7300 cm^{-1}. However, the infrared spectra recorded for Cr-doped mullite yielded no evidence for the presence of OH bands at 3650 cm^{-1}.

Tailing effects on the base line from the ultraviolet and infrared regions were approximated by locating Gaussian functions at 32900 and 3400 cm^{-1}. The correction from the infrared region was negligible. Absorption due to impurity ferrous ions was fitted by one Gaussian component, though strictly speaking it should be fitted by two Gaussian components, especially for large impurity levels (Ikeda, unpublished data). However, a one-component fit is sufficient for the very small Fe content of mullite. The mullite may have both ferric and ferrous ions, but the peak for ferric ions that is expected to appear at approx-

Table 2. Assignments of spectrum peaks to transitions and crystal-field parameters for chromium mullite

Transition	Al octahedra (cm^{-1})	Channel octahedra (cm^{-1})
$^4T_{1g}\leftarrow$	25300	22600
$^2T_{2g}\leftarrow$	—	—
$^4T_{2g}\leftarrow$	18850	15800
$^2T_{1g}\leftarrow$	—	—
$^2E_g \leftarrow {}^4A_{2g}$	—	—
10Dq	18850	15800
B	618	699
C	—	—
CFSE	22620	18960

TABLE 3. Octahedral mean M-O distances of Cr-doped mullite in comparison with those of Cr-free mullite

Octahedron type	Mean M-O distance of Cr-free mullite from structure refinement		Spectroscopic mean M-O distance of Cr-doped mullite: 1.982 Å (Based on spinel)		1.997 Å (Based on kosmochlor)	
			Fitness ratio in percentage			
			(Based on spinel)		(Based on kosmochlor)	
	A chain (Å)	B chain (Å)	A chain (%)	B chain (%)	A chain (%)	B chain (%)
S′	2.003	2.007	99.0	98.8	99.7	99.5
S	2.035	2.072	97.4	95.7	98.1	96.4
N	2.061	2.136	96.2	92.8	96.9	93.5
D	2.104	2.211	94.2	89.6	94.9	90.3
D′	2.143	2.286	92.5	86.7	93.2	87.4
M1	1.911 Å		100.2%		100.9%	

Note: Spectroscopic mean M-O distances were obtained after the fifth power rule, Equation 1 in the text. Each fitness ratio was obtained by dividing the spectroscopic mean M-O distance by the value from the structure refinement. Crystallographic mean M-O distances are based on data of Saalfeld and Guse (1981). Central positions were approximated in the following way for S and D octahedra: Midpoints of the base plane diagonals were connected. Then, the midpoints of this line and the top-bottom diagonal were connected in order to locate the approximate center as the midpoint of this final line (see also Fig. 6).

imately 22000 cm^{-1} (Ikeda, unpublished data) is not detectable because of the very low concentration of total Fe and superposition of such a peak with the observed major absorption peak. The standard deviation between the integrated fitting curves and the observed spectrum was 0.7%.

The Tanabe-Sugano secular equations for $3d^3$ configuration were applied for energy calculations (Tanabe and Sugano, 1954a, 1954b; Bates, 1962). The results confirm the presence of two sets of bands, one having higher energy than the other (18850 cm^{-1} instead of 15800 cm^{-1} in 10Dq values).

Discussion

Coordination polyhedra of Cr

Mean M-O distances around octahedral trivalent Cr ions can be estimated applying the following formula (White et al., 1971):

$$\Delta/\Delta' = (R'/R)^5 \quad (1)$$

where Δ and R denote 10Dq and the mean M-O distance for a standard specimen and Δ' and R' denote those for an unknown specimen. Values for standards were R = 1.926 Å (Smyth and Bish, 1988) and Δ = 18250 Å (Sviridov et al., 1973) for Cr-doped spinel ($MgAl_2O_4$) and R = 2.001 Å (Cameron et al., 1973) and Δ = 15640 cm^{-1} (Ikeda and Ohashi, 1974) for kosmochlor ($NaCrSi_2O_6$). They were considered to be representative of regular and irregular octahedra. The octahedral site symmetries are $D_{3d}(\bar{3}m)$ and $C_2(2)$, respectively. The assignment of the $^4T_{2g} \leftarrow {}^4A_{2g}$ transition of Cr^{3+} ions in kosmochlor given by Ikeda and Ohashi (1974) is incorrect. Revised crystal-field parameters are 15640, 645, and 2630 cm^{-1} for 10Dq, B, and C, respectively (Ikeda, unpublished data).

With respect to Δ and R values of the reference materials, the Cr^{3+} ions are most probably incorporated into the M1 octahedra, replacing Al^{3+} ions (Table 2). This assignment is reasonable according to the preference of Cr^{3+} ions for octahedral coordination. The Cr-containing M1 octahedra are relatively regular in shape, having point symmetry $C_{2h}(2/m)$, though a slight distortion from cubic symmetry $O_h(m3m)$ especially in the dipyramidal base is observed. The M1-O distances calculated from spectroscopic data on the basis of data for spinel and kosmochlor both fit well with observed distances, with fitness ratios of 100.2 and 100.9%, respectively. These values indicate a slight site expansion with substitution, with slightly better agreement on the basis of data for spinel (Table 3).

Geometry of channels

Rager et al. (1990) suggested that some of the Cr^{3+} ions in mullite are incorporated interstitially, possibly in the structural channels parallel to **c**. The frequent occurrence of O(C)* atoms instead of O(C) atoms may locally alter the straight structural channels. The normal cross section of uninterrupted channels is drawn in Figure 5a and designated as N, whereas Figures 5b and 5c give possible normal cross sections of channels at the altered positions. Obviously two kinds of cross sections occur as a result of the occurrence of O(C)* atoms, larger cross sections (D) and smaller ones (S). The S cross sections are associated with Al* tetrahedra.

The structural channels can also be viewed as bundles of chains of tetrahedra parallel to **c**, as shown in Figure 5. The corresponding chains of octahedra are designated as A (Figs. 5a–5c) and B (Figs. 5b and 5c) chains. There are six kinds of channel octahedra, three each of the A and B type:

1. Normal sized octahedra having displacements of O atoms in upper and lower vertices relative to ideal positions, designated as A(N) and B(N) octahedra, forming uninterrupted A and B chains, respectively, as seen in Figures 5a and 6.

2. Larger octahedra having displacements of O atoms in upper and lower vertices, designated as A(D) and B(D) octahedra, forming interrupted A and B chains with the normal sized octahedra, respectively, as seen in Figures 5c and 6.

3. Smaller octahedra having displacements of O atoms of upper and lower vertices, designated as A(S) and B(S) octahedra, forming interrupted A and B chains with the normal sized octahedra, respectively, as seen in Figures 5b and 6.

A and B octahedra have significantly different shapes as shown in Figure 6.

Spectroscopically determined mean M-O distances of

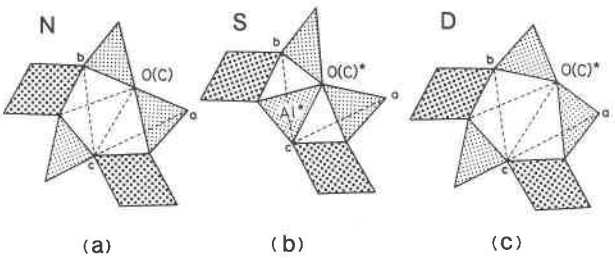

Fig. 5. Cross sections of structural channels in a view down the **c** axis. (**a**) N cross section (N = normal), (**b**) S cross section (S = interruption of the structural channels due to the presence of O(C)* forming Al* tetrahedron), (**c**) D cross section [D = local alteration of structural channels due to the presence of O(C)*].

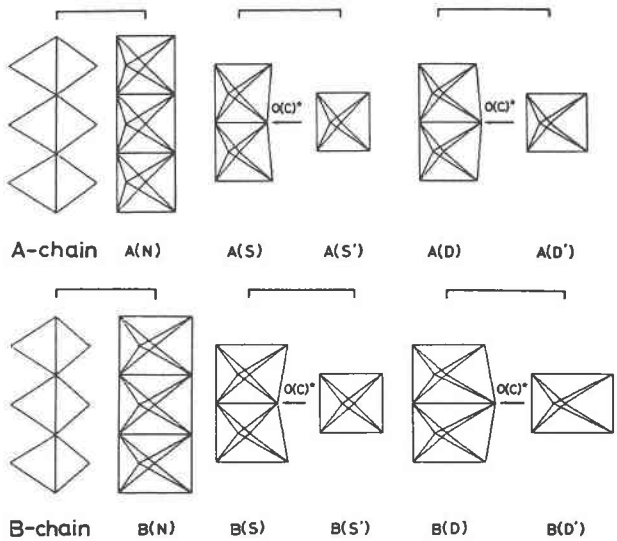

Fig. 6. Symmetries of channel octahedra. A(N) and B(N) octahedra on the left and the other octahedra in the middle and on the right. S′ and D′ octahedra require coupling with S and D octahedra in order to form A and B chains.

channel octahedra as obtained applying formula 1 are listed in Table 3. Mean M-O distances calculated from data for the structure of Cr-free mullite (Saalfeld and Guse, 1981) are also listed. Comparison between the spectroscopically determined mean M-O distances and those from the structure refinement yields various fitness ratios as given in Table 3 in percentages. Obviously, the results for B(S) and especially of A(S) octahedra fit best. However, a considerable discrepancy from 100% still exists. An improvement can be achieved by the presence of two or more successive O(C)* atoms in the mullite structure, resulting in smaller octahedra [A(S′) and B(S′) octahedra] and larger octahedra [A(D′) and B(D′) octahedra], all having rectangular base planes (Fig. 6). It should be noted that these octahedra do not exist in the normal mullite structure, but the structure is flexible enough to accommodate their topology. Spectroscopically calculated mean M-O distances are in good accordance with mean values for A(S′) and B(S′) octahedra as determined from structure refinement (Table 3). Slightly smaller fitness values indicate a small contraction of the channel sites when Cr is incorporated. Kosmochlor-based data give better results, although the difference between those of kosmochlor and spinel is slight.

Probable site occupancies and CFSE

Site occupancy distributions of Cr between M1 octahedra and channel octahedra have been estimated from integrated intensities of the two main bands, $({}^4T_{2g} \leftarrow {}^4A_{2g}) + ({}^4T_{1g} \leftarrow {}^4A_{2g})$, assuming that transition probabilities between the two sites are identical. Simple comparison yields 40 and 60% occupancy of M1 octahedra and channel octahedra, respectively. Ground-state trivalent Cr ions are not Jahn-Teller species, and large site distortions that affect the transition probabilities significantly cannot be considered for the Cr positions in the mullite structure. That is, the predicted distortions in structure provide a reasonable environment for Cr ions. As a consequence, the inferred relative occupancies may be accurate.

A large difference of CFSE was observed at room temperature for Cr^{3+} occurring in M1 octahedra and channel octahedra (Table 2), showing a CFSE gap of 3660 cm^{-1} for the two sites. If Cr^{3+} ions enter either A(S′) octahedra or B(S′) octahedra, the observed CFSE preferential energy of M1 octahedra cannot be explained. It may be concluded that Cr^{3+} ions enter A(S′) and B(S′) octahedra. This means that the mullite structure contains three nonequivalent octahedral Cr^{3+} sites, i.e., M1 octahedra, A(S′) octahedra, and B(S′) octahedra. It is estimated that there is at most only a CFSE gap of 480 cm^{-1} for the two nonequivalent channel octahedra. Therefore, nearly equal distribution of Cr^{3+} ions may occur between the two kinds of channel octahedra. If Cr ions are equally distributed between A(S′) octahedra and B(S′) octahedra, the relative occupancies of the three nonequivalent octahedra are 40, 30, and 30%, respectively. This is in accordance with the order of CFSE preference.

In a study of Cr-bearing diopside of the $CaMgSi_2O_6$-$CaCrCrSiO_6$ and $CaMgSi_2O_6$-$CaCrAlSiO_6$ series (Ikeda and Yagi, 1977, 1982), an average CFSE gap of only 700 cm^{-1} was found for trivalent octahedral high spin Cr and trivalent tetrahedral low spin Cr. Accordingly, the 3660-cm^{-1} gap observed for the M1 octahedra and the channel octahedra in Cr-bearing mullite is not too small. The octahedral CFSE preference energy of 4340 cm^{-1} lies between those of $^{[6]}Cu^{2+}$ and $^{[4]}Cu^{2+}$ in $CuAl_2O_4$ spinel. Reed (1973) considered that Madelung and short-range energies reduce the magnitude of the octahedral preference energy. The same consideration may be applicable to Cr-doped mullite.

Recently, Wojtowicz et al. (1988), Wojtowicz and Lempicki (1988), Knutson et al. (1989), and Liu et al. (1990) carried out spectroscopic studies on Cr-containing ($\leqq$0.05 wt% Cr) mullite glass ceramics. The mullite glass

ceramics had glassy matrices with chemical compositions different from those of the mullite crystallites, whereas the present mullite sample is glass free. The chemical composition of these materials was also quite different, including B_2O_3 and other components. Crystal-field spectra were similar to those of this study. Knutson et al. (1989) found high-field and low-field sites for trivalent Cr. The former may correspond to the M1 site discussed in this study. However, we do not believe that this should be attributed to the occurrence of Cr in the glass phase alone. The low-field site may include the channel sites discussed in this study, although thermal history and chemical composition of the samples are different from those of our sample.

Conclusions

Trivalent Cr ions are incorporated into M1 octahedra of mullite, substituting for Al^{3+}. Moreover, Cr^{3+} may occur in interstitial octahedral sites in the structural channels of mullite.

Comparison of mean M-O distances calculated on the basis of spectroscopic measurement with those calculated on the basis of X-ray structure refinements revealed the presence of two kinds of vacant octahedra in the channels that are suitable for Cr^{3+} incorporation. These are the A(S′) octahedra and B(S′) octahedra of the structure. Formation of such octahedra requires the presence of two or more successive O(C)* atoms.

The presence of Cr^{3+} in the M1 octahedra and in channel octahedra can be distinguished by means of crystal-field spectra curve fittings, resulting in two sets of spectra. One set, which is assigned to channel Cr^{3+} octahedra, is inferred to be due to superposition of two peaks. These spectra cannot easily be resolved because of the proximity of absorption bands having, at most, only a difference of 400-cm^{-1} 10Dq. Therefore, the analysis of crystal-field spectra was carried out without distinction of the superimposed bands.

Consideration of CFSE between M1 octahedra and channel octahedra also supports the three-site occupation by Cr^{3+} ions. That is, if Cr^{3+} substitutes in M1 octahedra and only one kind of channel octahedron, the observed CFSE preference energy of M1 octahedra cannot be maintained as 3660 cm^{-1}. Resolution of this problem is provided by Cr^{3+} ions in three sites, i.e., in M1 octahedra, A(S′) octahedra, and B(S′) octahedra.

Integrated absorption intensities yield estimated Cr^{3+} site occupancies of approximately 40, 30, and 30% in M1, A(S′), and B(S′) octahedra, respectively. Based on data from structure refinement, the atomic coordinates of Cr are (0,0,0), (0.20,0.51,0), and (0.10,0.26,0) for the M1, A(S′), and B(S′) octahedra, respectively.

Acknowledgments

K.I. and M.A. express their gratitude to K. Matsubara of Yamaguchi University and Y. Matsunaga of Hokkaido University for use of the spectrophotometer facilities. Thanks are also due to T. Koyanagi for the measurement of spectra and to T. Sakao for typing the manuscript. The present study was financially supported by grant 02640631 from the Ministry of Education of the Japanese government. H.S. and H.R. thank H. Krause for technical assistance and the German Research Foundation (DFG) for financial support.

References cited

Angel, R.J., and Prewitt, C.T. (1987) The incommensurate structure of mullite by Patterson synthesis. Acta Crystallographica, B43, 116–126.

Aramaki, S., and Roy, R. (1962) Revised phase diagram for the system Al_2O_3-SiO_2. Journal of the American Ceramic Society, 45, 229–242.

Bates, T. (1962) Ligand field theory and absorption spectra of transition metal ions in glasses. In J.D. Mackenzie, Ed., Modern aspects of the vitreous state, vol. 2, p. 195–254. Butterworths, London.

Beales, K.J., and Day, C.R. (1980) A review of glass fibres for optical communications. Physics and Chemistry of Glasses, 21, 5–33.

Burnham, C.W. (1963) The crystal structure of mullite. Carnegie Institution of Washington Year Book, 62, 158–165.

Burns, R.G. (1972) Mineralogical applications of crystal field theory, 224 p. Uchidarokakuho-shinsha, Tokyo (in Japanese).

Cameron, M., Sueno, S., Prewitt, C.T., and Papike, J.J. (1973) High temperature crystal chemistry of acmite, diopside, hedenbergite, jadeite, spodumene, and ureyite. American Mineralogist, 58, 594–618.

Cameron, W.E. (1977) Composition and cell dimensions of mullite. Journal of the American Ceramic Society Bulletin, 56, 1003–1011.

Durovič, S. (1969) Refinement of the crystal structure of mullite. Chemicke Zvesti, 23, 113–128.

Earnshaw, A. (1970) Introduction to magnetochemistry, 148 p. Baifukan, Tokyo (in Japanese).

Figgis, B.N. (1969) Introduction to ligand fields, 340 p. Nankodo, Tokyo (in Japanese).

Goldman, D.S., and Rossman, G.R. (1977) The identification of Fe^{2+} in the M(4) site of calcic amphiboles. American Mineralogist, 62, 205–216.

Hariya, Y., Dollase, W.A., and Kennedy, G.C. (1969) An experimental investigation of the relationship of mullite to sillimanite. American Mineralogist, 54, 1419–1441.

Ikeda, K., and Ohashi, H. (1974) Crystal field spectra of diopside-kosmochlor solid solutions formed at 15kb pressure. The Journal of the Japanese Association of Mineralogists, Petrologists, and Economic Geologists, 69, 103–109.

Ikeda, K., and Yagi, K. (1977) Experimental study on the phase equilibria in the join $CaMgSi_2O_6$-$CaCrCrSiO_6$ with special reference to the blue diopside. Contributions to Mineralogy and Petrology, 61, 91–106.

——— (1982) Crystal-field spectra for blue and green diopsides synthesized in the join $CaMgSi_2O_6$-$CaCrAlSiO_6$. Contributions to Mineralogy and Petrology, 81, 113–118.

Kettle, S.F.A. (1972) Coordination compounds, 267 p. Baifukan, Tokyo (in Japanese).

Klug, F.J., Prochazka, S., and Doremus, R.H. (1990) Alumina-silica phase diagram in the mullite region. Ceramic Transactions, 6, 15–43.

Knutson, R., Liu, H., and Yen, W.M. (1989) Spectroscopy of disordered low-field sites in Cr^{3+}: Mullite glass ceramic. Physical Review B, 40, 4264–4270.

Liu, H., Knutson, R., Jia, W., Strauss, E., and Yen, W.M. (1990) Spectroscopic determination of the distribution of Cr^{3+} sites in mullite ceramics. Physical Review B, 41, 12888–12894.

McConnell, J.D.C., and Heine, V. (1985) Incommensurate structure and stability of mullite. Physical Review B, 31, 6140–6142.

Morimoto, N. (1990) Modulated structure and vacancy ordering in mullite. Ceramic Transactions, 6, 115–124.

Pask, J.A. (1990) Critical review of phase equilibria in the Al_2O_3-SiO_2 system. Ceramic Transactions, 6, 1–13.

Rager, H., Schneider, H., and Graetsch, H. (1990) Chromium incorporation in mullite. American Mineralogist, 75, 392–397.

Reed, J.S. (1973) Optical spectra of Cu^{2+} and Ni^{2+} in intermediate aluminate spinels. Journal of the American Ceramic Society, 56, 525–527.

Saalfeld, H. (1979) The domain structure of 2:1-mullite ($2Al_2O_3 \cdot SiO_2$). Neues Jahrbuch für Mineralogie Abhandlungen, 134, 305–316.

Saalfeld, H., and Guse, W. (1981) Structure refinement of 3:2-mullite ($3Al_2O_3 \cdot 2SiO_2$). Neues Jahrbuch für Mineralogie Monatshefte, 4, 145–150.

Sadanaga, R., Tokonami, M., and Takéuchi, Y. (1962) The structure of mullite, $2Al_2O_3 \cdot SiO_2$, and relationship with the structures of mullite and andalusite. Acta Crystallographica, 15, 65–68.

Schneider, H. (1986) Formation, properties and high-temperature behaviour of mullite, 148 p. Habilitationsschrift, Faculty of Chemistry, University of Münster, Münster, Germany.

——— (1990) Transition metal distribution in mullite. Ceramic Transactions, 6, 135–158.

Smyth, J.R., and Bish, D.L. (1988) Crystal structures and cation sites of the rock-forming minerals, 332 p. Allen & Unwin, Winchester, England.

Sviridov, D.T., Sevastyanov, B.K., Orekhova, V.P., Sviridova, R.K., and Veremeichik, T.F. (1973) Optical absorption spectra of excited Cr^{3+} ions in magnesium spinel at room and liquid nitrogen temperatures. Optics and Spectroscopy, 35, 102–107.

Tanabe, Y., and Sugano, S. (1954a) On the absorption spectra of complex ions I. Journal of the Physical Society of Japan, 9, 753–766.

——— (1954b) On the absorption spectra of complex ions II. Journal of the Physical Society of Japan, 9, 766–779.

White, W.B., McCarthy, G.J., and Scheetz, B.E. (1971) Optical spectra of chromium, nickel, and cobalt-containing pyroxenes. American Mineralogist, 56, 72–89.

Wojtowicz, A.J., and Lempicki, A. (1988) Luminescence of Cr^{3+} in mullite transparent glass ceramics (II). Journal of Luminescence, 39, 189–203.

Wojtowicz, A.J., Meng, W., Lempicki, A., Beall, G.H., and Hall, J.W. (1988) Spectroscopic characterization of Cr doped mullite glass-ceramics. IEEE Journal of Quantum Electronics, 24, 1109–1113.

Manuscript received March 21, 1991
Manuscript accepted October 14, 1991